Systems & Control Transactions

Original Research Article
Peer Reviewed Conference Proceeding
ESCAPE 36 - European Symposium on Computer Aided Process Engineering
Sheffield, UK. 21-24 June 2026

PSE PRESS

Temporal aggregation bias in model-based Direct Air Capture performance under weather variability

Eleni Chalasti[abc], Gbemi Oluleye[bc], Maria M. Papathanasiou[ab], Ronny Pini[ab]*

[a] Imperial College London, Department of Chemical Engineering, London, United Kingdom
[b] Imperial College London, Sargent Centre for Process Systems Engineering, London, United Kingdom
[c] Imperial College London, Grantham Institute - Climate Change and the Environment, London, United Kingdom
* Corresponding Author: rpini@imperial.ac.uk.

ABSTRACT

Direct Air Capture (DAC) is a negative emissions technology whose performance is inherently linked to ambient conditions, which directly affect its primary feed stream (air). A common simplification in DAC model simulations is the use of fixed weather conditions, which can bias the predicted performance under weather variability. In response, this study quantifies the impact of local meteorological variability and temporal weather aggregation on the performance of DAC units. Building on a previously developed and validated 1D mechanistic model of a fixed-bed Steam-assisted Temperature Vacuum Swing Adsorption (S-TVSA) DAC process, we simulate its operation using weather data from the Met Office station at Buchan (UK), near the Saint Fergus terminal - a strategic hub for Carbon Capture and Storage (CCS) activities in Scotland. A two-branch methodological framework is developed combining optimization and forward simulations. Operating conditions are optimized using a multi-objective genetic algorithm (NSGA-II) to maximize productivity (Pr) and minimize specific equivalent work (Weq) at two temporal resolutions. Furthermore, daily weather inputs are aggregated on a monthly and yearly scale to assess the impact of data resolution on model predictions and real operational gains. Results show that temporal weather aggregation to yearly averages biases DAC key performance indicators, overestimating Pr by up to 5% while underestimating Weq by up to 31%, relative to performance based on daily weather variations. Moreover, optimization strategies that explicitly account for monthly weather variability present monthly gains, by increasing Pr by up to 10%. Yet, these monthly gains do not necessarily translate into significant operational performance benefits at the annual scale when daily weather data is propagated in the process model.

Keywords: Carbon Capture, Process Design, Adsorption, Dynamic Modelling, Genetic Algorithm, United Kingdom, Industrial Clusters, Direct Air Capture, Temporal Weather Aggregation

INTRODUCTION

In light of the ongoing need to pursue mitigation pathways towards climate change, consistent with the Paris Agreement targets, Direct Air Capture (DAC) has emerged as a carbon dioxide (CO_2) removal (CDR) option capable of delivering negative emissions by counterbalancing legacy emissions and hard-to-abate residual industrial CO_2 that cannot be eliminated through conventional abatement measures [1]. DAC is a novel yet technically complex CDR technology during which atmospheric CO_2 is artificially removed through an engineered air contactor [2]. Unlike point-source capture technologies, DAC targets the dilute CO_2 in ambient air and is intrinsically sensitive to local weather conditions [3]. Furthermore, although DAC systems are claimed to be location-independent, their operation depends on the availability and integration of utilities, land and energy sources. To avoid the need for building new DAC-specific infrastructure and to reduce their energy consumption, the integration of DAC systems within existing industrial clusters is a beneficial engineering solution. In fact, co-locating DAC units near existing industrial sites can enhance the overall efficiency of the system thanks to the availability of suitable, existing infrastructure, available waste utilities (heat, cooling water) and low likelihood of

environmental constraints [1].

Despite ongoing, promising momentum, the widespread adoption of DAC as a viable CDR at large-scale is currently constrained by several interrelated, unresolved technical complexities that include the integration of resources within existing industrial activity [1], [3], high cost of capture [4], [5], and performance uncertainties due to operational variability under real-world conditions [3], [4], [6].

Dynamic process simulations have highlighted the sensitivity of DAC performance to ambient weather, including spatiotemporal variations in energy demand driven by different temperature (T) and relative humidity (RH) profiles across different locations [4], [7]. To the best of the authors' knowledge, only few studies have quantified the impact of fine weather variability and temporal aggregation on technical key performance indicators (KPIs) [3], [6], [8], employing optimization approaches ranging from mixed-integer linear programming (MILP) to data-driven surrogate-based branch-and-bound (DDSBB) and Bayesian optimization. Most DAC studies report performance under a limited set of representative conditions or rely on temporally averaged weather inputs, without constructing year-long dynamic performance profiles that resolve intra-annual variability. Consequently, the impact of variable ambient conditions on deviations from design-point operation - particularly near constraint limits and along energy-productivity trade-offs - remains insufficiently quantified. In addition, DAC is often assessed in isolation from region-specific deployment constraints such as industrial geography, local climate, and evolving CO_2 transport-and-storage (T&S) infrastructure.

To address this gap, we take an initial step toward a decision-support framework for DAC siting using the UK as a case study. We evaluate a Steam-assisted Temperature-Vacuum Swing Adsorption (S-TVSA) fixed-bed process for DAC at an industrial UK location and develop dynamic performance profiles under off-design ambient conditions. We compare predictions obtained using different weather resolutions to quantify temporal aggregation bias, and we optimize operating variables using NSGA-II to maximize productivity (Pr) and minimize specific equivalent work (Weq) under capture-grade specifications. Finally, we quantify the value of higher optimization resolution by comparing a single yearly optimization against twelve month-specific optimizations accounting for intra-annual variability.

METHODOLOGY

Temperature-Vacuum-Swing Adsorption Cycle

Previous work focused on the development of a high-fidelity mechanistic model in MATLAB to simulate and optimize the performance of an S-TVSA DAC unit, which constitutes the modeling basis for this work [2]. The system separates CO_2 from ambient air containing 400 ppm CO_2, nitrogen (N_2), and water vapor (H_2O) at atmospheric pressure (1 bar) and local ambient temperature, using the benchmark adsorbent APDES-NFC. It comprises five sequential steps: (i) adsorption, (ii) blowdown, (iii) heating, (iv) desorption, and (v) pressurization, as shown in Figure 1. Each step operates under a distinct set of conditions, ranging from low pressure (P) and temperature (P_L, T_L) to high pressure and temperature (P_H, T_H). During adsorption, CO_2 is selectively captured while H_2O co-adsorbs on the sorbent's surface. During blowdown, pressure is reduced to vacuum to remove residual N_2. Steam-assisted heating under vacuum promotes the desorption step, producing a CO_2/H_2O stream which is separated downstream by condensation. At the last step, the bed is then repressurized to initiate the next cycle using air and cooling water.

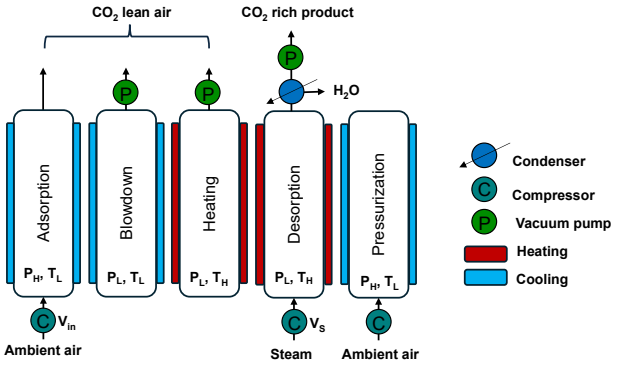


Figure 1. Schematic representation of the 5-step S-TVSA cycle considered in this study.

The high-fidelity, one dimensional (1D) fixed bed model describes competitive CO_2/H_2O adsorption equilibria as functions of pressure, temperature, and gas composition using thermodynamically consistent isotherm models (GAB for H_2O and modified Toth for CO_2 [9]), assuming negligible N_2 adsorption. Adsorption dynamics are captured by coupled partial differential equations for mass, energy, and momentum balances with axial dispersion. Intraparticle mass transfer is captured using a Linear Driving Force (LDF) approximation. The cycle is simulated until cyclic steady state is reached, defined by <0.5% variation in state variables between consecutive cycles at all axial locations.

Multi-objective optimization

The multi-objective optimization problem to minimize Weq and maximize Pr, subject to a product purity constraint (s.t. Pu $\geq$ 95%) is formulated as shown below:

$$\min(-Pr + \varphi, W_{eq} + \varphi) \quad (1)$$

$$s.t\ \theta_L \le \theta \le \theta_U$$

$$\varphi = 0.25 \times [\max(0, 95 - Pu)]^2$$

where θ is the vector of process operating variables, bounded between a lower (θ_L) and upper (θ_U) value as shown in Table 1. The equivalent work term represents the total energy duty of the system, combining the thermal (heating, steam purge) and electrical energy requirements (compressor, vacuum pump, condenser) into a single metric [2].

Table 1. Upper and lower bounds applied to the operating variables θ for optimization of the S-TVSA process.

	t_{ads} (s)	t_{heat} (s)	t_{des} (s)	P_L (Pa)	T_H (K)	v_s (m/s)	v_{in} (m/s)
θ_L	1,000	500	1,000	500	363	0.0015	0.005
θ_U	15,000	1,500	40,000	5,000	373	0.005	0.01

Building on previous work, the purity constraint is represented as a quadratic loss penalty function with a drawdown coefficient c = 0.25 [2]. The decision variables that are optimized include the adsorption time (t_{ads}), the heating time (t_{heat}), the desorption time (t_{des}), the vacuum pressure (P_L), the steam temperature (T_H), the steam velocity (v_s), and the air feed velocity (v_{in}). The duration of the blowdown (t_{bd}) and the pressurization (t_{pres}) steps is 30s [2].

Industrial Clusters – Location case-study selection

To enable a cluster-specific assessment and the construction of a year-long dynamic performance profile under realistic ambient conditions, a representative site within the Scottish Industrial Cluster was selected. The Scottish Cluster is particularly relevant for large-scale DAC deployment due to its proximity to existing and planned CO_2 transport and storage infrastructure [10]. The area of Saint Fergus was chosen as a reference location, serving as a proxy for cluster-level deployment and enabling a detailed, high-resolution assessment of weather-driven performance variability. Year-long ambient meteorological data for 2024 (T_d, RH_d) were obtained on a daily resolution from the Buchan station, the nearest UK Met Office station to the selected reference site [11].

Effect of weather variability and temporal aggregation

Dynamic Performance Profiles

Previous DAC process-modelling studies have typically employed constant ambient conditions to evaluate system performance. Although computationally efficient, this assumption neglects the intrinsic temporal variability of atmospheric T and RH that directly define DAC inlet conditions and may therefore bias predicted KPIs. To systematically evaluate the impact of weather resolution on DAC performance, we develop a two-branch methodological framework combining optimization and forward simulations under different temporal representations of ambient conditions. By developing dynamic performance profiles, we can quantify how real operation at a fixed operating set of conditions (fixed operating strategy) responds to different temporal resolutions of weather.

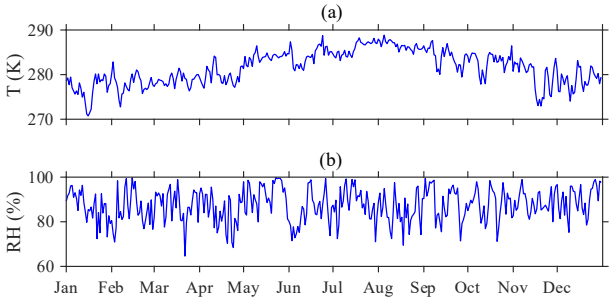


Figure 2. Daily ambient conditions at Buchan in 2024: (a) temperature T_d (K) and (b) relative humidity RH_d (%). Over the year, T_d ranged from 270.8-288.9 K and RH_d from 64.6-99.8%. Annual mean values were $\bar{T}_y = 281.6$ K and $\overline{RH}_y = 87.4\%$.

Furthermore, we can evaluate whether temporal aggregation of weather data yields values that are consistent with the fixed monthly and yearly inputs commonly assumed in DAC process simulations, and quantify any discrepancies introduced by this simplification. Daily weather data (T_d, RH_d) for the chosen location, with $d \in \{1, \dots, D\}$ where D are the number of days in 2024 (366), are obtained directly from the data source. The first step of the workflow involves running a multi-objective optimization under yearly averaged $(\bar{T}_y, \overline{RH}_y)$ conditions. From the resulting Pareto set, as shown in Figure 3, the maximum-productivity point $(\mathrm{Pr}^*_{y,max})$ is selected to define the fixed operating strategy for this workflow. Next, this fixed vector of decision variables, θ^*_y, that describe optimal operating conditions at $\mathrm{Pr}^*_{y,max}$ is propagated into forward simulations in the DAC model using the full sequence of daily weather inputs (T_d, RH_d). This procedure yields time-dependent daily trajectories of KPIs, enabling a direct correlation between ambient weather inputs and DAC performance. Daily weather inputs are averaged on a monthly and yearly basis as shown below:

$$\bar{T}_{m,i} = \frac{1}{D_{m,i}} \sum_{d=1}^{D_{m,i}} T_d \qquad (2)$$

$$\overline{\mathrm{RH}}_{m,i} = \frac{1}{D_{m,i}} \sum_{d=1}^{D_{m,i}} RH_d \tag{3}$$

$$\bar{T}_y = \frac{1}{\mathrm{D}} \sum_{d=1}^{\mathrm{D}} T_d \tag{4}$$

$$\overline{\mathrm{RH}}_y = \frac{1}{\mathrm{D}} \sum_{d=1}^{\mathrm{D}} RH_d \tag{5}$$

$D_{m,i}$ denotes the number of days in month i.

Forward Simulations

To assess the impact of weather data temporal resolution on performance predictions, the daily KPI outputs are aggregated into monthly and yearly values.

$$\overline{KPI}_{m,i} = \frac{1}{D_{m,i}} \sum_{d=1}^{D_{m,i}} KPI_d(T_d, RH_d, \theta_y^*) \tag{6}$$

$$\overline{KPI}_y = \frac{1}{\mathrm{D}} \sum_{d=1}^{\mathrm{D}} KPI_d(T_d, RH_d, \theta_y^*) \tag{7}$$

The resulting averaged KPIs are then compared against KPIs obtained from simulations that use fixed monthly $(KPI_{m,i}(\bar{T}_{m,i}, \overline{RH}_{m,i}, \theta_y^*))$ and fixed yearly $(KPI_y^*(\bar{T}_y, \overline{RH}_y, \theta_y^*))$ ambient conditions by testing the following null hypotheses H_0.

$$H_0: \overline{KPI}_{m,i} - KPI_{m,i}(\bar{T}_{m,i}, \overline{RH}_{m,i}, \theta_y^*) = 0 \tag{8}$$

$$H_0: \overline{KPI}_y - KPI_y^*(\bar{T}_y, \overline{RH}_y, \theta_y^*) = 0 \tag{9}$$

In addition, we can also estimate yearly average KPIs using weighted fixed-month simulations:

$$\bar{\overline{KPI}}_y = \sum_{i=1}^{12} \frac{D_{m,i}}{D} KPI_{m,i}(\bar{T}_{m,i}, \overline{RH}_{m,i}, \theta_y^*) \tag{10}$$

This methodology allows us to (i) determine whether the temporal averaging implied in fixed-weather modelling is valid and (ii) to quantify the operational penalties that arise when a DAC unit optimized for nominal yearly conditions is exposed to real atmospheric variability.

Process Optimization

The second branch of the workflow will allow us to quantify the effect of temporal resolution in process improvements of DAC optimal performance. We solve the optimization problem using NSGA-II under two temporal representations of ambient conditions: yearly constant conditions as described above $(\bar{T}_y, \overline{RH}_y)$ and monthly-constant conditions $(\bar{T}_{m,i}, \overline{RH}_{m,i})$, yielding 12 different sets of decision variables $(\theta_{m,i}^*)$. For each optimization scenario, two representative Pareto solutions are extracted: the maximum Pr $(\mathrm{Pr}_{y,max}^*)$ and the minimum Weq points $(\mathrm{Weq}_{y,min}^*)$. For the monthly optimization case, annual mean KPIs are computed by averaging weighted monthly optima:

$$\bar{\overline{\mathrm{KPI}}}_y^* = \sum_{i=1}^{12} \frac{D_{m,i}}{D} KPI_{m,i}^*(\bar{T}_{m,i}, \overline{RH}_{m,i}, \theta_{m,i}^*) \tag{11}$$

This branch of the workflow tests whether increasing the temporal resolution of the optimization inputs leads to improved predicted annual-mean optimal performance relative to a single yearly-constant optimization. To this end, the following null hypothesis is tested:

$$H_0: KPI_y^*(\bar{T}_y, \overline{RH}_y, \theta_y^*) - \bar{\overline{\mathrm{KPI}}}_y^*(\bar{T}_{m,i}, \overline{RH}_{m,i}, \theta_{m,i}^*) = 0 \tag{12}$$

Furthermore, to quantify the month-specific value of re-optimization, we compare the performance obtained when operating each month using the annually optimal decision vector (θ_y^*) against the performance achieved under month-optimal settings $(\theta_{m,i}^*)$, both evaluated under the same month-averaged ambient conditions $(\bar{T}_{m,i}, \overline{RH}_{m,i})$. This test isolates the operational benefit attributable solely to adjusting operating parameters at a monthly timescale, relative to maintaining fixed yearly operation:

$$H_0: KPI_{m,i}(\bar{T}_{m,i}, \overline{RH}_{m,i}, \theta_y^*) - KPI^*{}_{m,i}(\bar{T}_{m,i}, \overline{RH}_{m,i}, \theta_{m,i}^*) = 0 \tag{13}$$

Aggregated on an annual scale, we also evaluate:

$$H_0: \bar{\overline{KPI}}_y - \bar{\overline{\mathrm{KPI}}}_y^* = 0 \tag{14}$$

Finally, to evaluate whether gains identified under aggregated ambient conditions translate into improved annual operation under fully time-resolved weather, we test the following null hypothesis:

$$H_0: \overline{KPI}_y - \overline{KPI_y^*} = 0 \tag{15}$$

, where we define:

$$\overline{KPI_y^*} = \frac{1}{\mathrm{D}} \sum_{d=1}^{\mathrm{D}} KPI_d(T_d, RH_d, \theta_{m,i}^*) \tag{16}$$

RESULTS

Dynamic Performance Profiles

The DAC unit was optimized at nominal weather conditions that correspond to the yearly average. From the resulting Pareto Front shown in Figure 3, the combination of operating variables corresponding to the maximum productivity was chosen to create our fixed operating strategy.

The simulated DAC productivity exhibits intra-annual variability (Figure 4b), ranging from 5.6 to 6.2 kg/m^3/day, with lower values occurring under combinations of high RH and medium-to-high ambient T. Although modest in magnitude, a non-uniform productivity profile can propagate across the CO_2 removal value chain. At plant level, it can reduce capacity utilization and

can bias sizing when designs rely on annual-average performance. At cluster scale, time-varying CO_2 output may undermine steady-supply assumptions for downstream compression, transport, and storage infrastructure, lowering utilization of shared assets. Even without explicitly modeling the Carbon Capture & Storage (CCS) chain in this study, these results suggest that sustained productivity fluctuations can materially affect integration, cost estimates, and deployment robustness. Energy consumption (Figure 4c) is strongly affected, displaying peak-to-trough variations of up to 76% over the year - an effect that is obscured when steady-state or temporally averaged conditions are assumed. It is interesting to notice that high RH values cause a simultaneous increase in energy consumption and reduction in productivity, consistent with CO_2-H_2O co-adsorption: at very humid conditions, H_2O adsorption dominates and water-loaded sorption sites require additional regeneration, increasing energy requirements while reducing effective CO_2 throughput. Finally, purity shows a clearer intra-annual trend, decreasing during summer months (Figure 4a). This is consistent with the decreasing adsorption capacity and sorbent's reduced selectivity at higher temperatures, which gives more space for H_2O to compete by occupying and accumulating on the void spaces, yielding a mixture which is less rich in CO_2. Although the purity constraint of 95% was met for this combination of ambient conditions and marginal peak-to-through variability (1%) was observed, variable product purity can entail the risk of increasing downstream processing costs to maintain the stream within spec, with significant impacts on the downstream CCS chain.

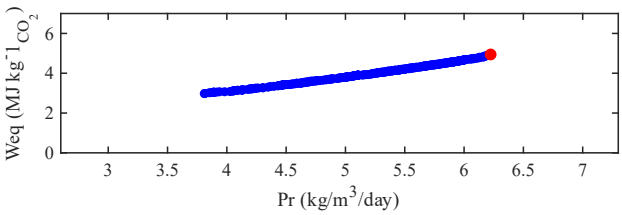


Figure 3. Pareto Front resulting from the multi-objective optimization problem of maximizing productivity (Pr) and minimizing equivalent work (Weq) using NSGA-II.

Temporal Weather Averaging

Figure 5 compares normalized DAC performance indicators obtained using different temporal representations of ambient conditions while maintaining a fixed operating strategy (θ_y^*). KPIs calculated using yearly average conditions are included as a reference (dashed lines) to reflect the common simplifying assumption adopted in much of the existing DAC modeling literature. The results demonstrate that the use of temporally averaged weather inputs leads to systematically biased performance predictions. When monthly- (green bins) or yearly-averaged (dashed line) T and RH values are employed, KPIs can be either over- or under-estimated relative to simulations driven by daily resolved meteorological data (purple bins). System productivity is consistently overestimated, while energy requirements are significantly underestimated when constant yearly ambient conditions are assumed.

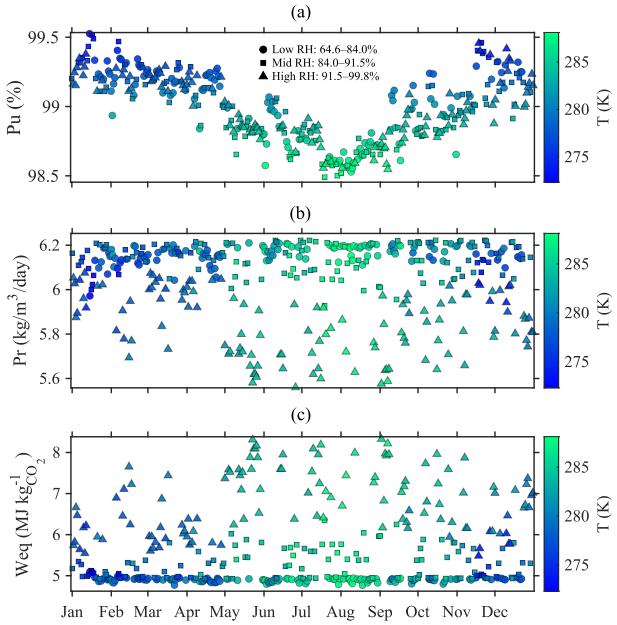


Figure 4. Dynamic annual profiles of (a) purity (Pu), (b) productivity (Pr), and (c) equivalent work (Weq) for the optimized DAC unit operating at St. Fergus.

May corresponds to the maximum deviation from the yearly nominal operating conditions, with productivity overpredicted by up to 5% and energy demand underestimated by approximately 31% when compared to the daily-resolved cases. Despite these discrepancies, CO_2 purity is shown to be comparatively insensitive to temporal aggregation, with deviations remaining below 1% across all cases. This indicates that purity constraints are robust to weather averaging for the operating regime considered. Other critical KPIs exhibit much stronger nonlinear responses to ambient variability. Electrical energy consumption is underestimated by up to 195% when yearly fixed temporal representations are used underscoring the extent to which averaging suppresses high-energy operating periods. On an annual scale (purple bins), the same trends are observed compared to the yearly-averaged simulations (dashed line). This discrepancy highlights that the annual mean of a nonlinear KPI does not correspond to the indicator evaluated at annual-mean ambient conditions. Hence, we show that:

$$\overline{KPI}_y \neq KPI_y^*(\bar{T}_y, \overline{RH}_y, \theta_y^*)$$

A similar effect is observed at the monthly level. When KPIs obtained from daily-resolved simulations (light purple bins) are averaged over each month and compared to simulations performed using fixed monthly-average ambient conditions (green bins), systematic deviations persist. Specifically, while purity remains largely unaffected, productivity is overestimated by up to 2.5% and energy consumption is underestimated by up to 11% depending on the month. Hence, we conclude that:

$$\overline{KPI}_{m,i} \neq KPI_{m,i}(\bar{T}_{m,i}, \overline{RH}_{m,i}, \theta_y^*)$$

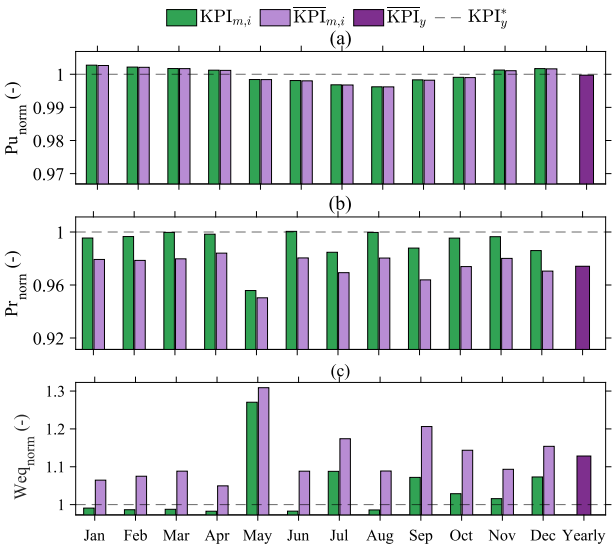


Figure 5. Comparison of normalized (a) purity (Pu_{norm}), (b) productivity (Pr_{norm}), and (c) equivalent work (Weq_{norm}) obtained at different temporal resolutions. All results are obtained using the same operating variables θ_y^* and are normalized by the nominal case that produces KPI_y^*.

These deviations arise because short-term excursions to unfavorable temperature and humidity conditions - particularly those associated with high energy penalties - are smoothed out when average inputs are used. These findings demonstrate that temporal aggregation masks the true operational variability of DAC systems by suppressing extreme but impactful weather conditions. While low-resolution weather data may be sufficient for predicting product quality, it fails to accurately capture energy requirements and the system's productivity. This has important implications for techno-economic assessments, utility sizing, and system integration studies, where underestimating peak and cumulative energy demand may lead to overly optimistic cost projections and misinformed process design.

Optimization at temporal resolutions

Building on the forward-simulation analysis, we move to the optimization framework which enables detangling (i) the benefit of re-optimizing operating conditions at a monthly timescale, (ii) the month- and yearly specific improvement achievable relative to fixed annual operation, and (iii) the extent to which apparent gains under aggregated weather inputs translate into improved performance under fully time-resolved (dynamic) ambient conditions. These hypotheses provide a structured basis to determine whether increasing temporal resolution yields meaningful operational improvements, or whether it primarily increases computational burden without material gains in annual performance. As seen in Table 2, monthly re-optimization ($\overline{\text{KPI}}_y^*$) does not yield consistent annual-mean performance gains relative to a single yearly-constant optimization (KPI_y^*). At $Pr_{y,max}^*$, monthly optimization produces negligible change in productivity but increases equivalent work from 4.95 to 5.16 (+4.35%), indicating a deterioration in energy performance. In contrast, at $Weq_{y,min}^*$, monthly optimization substantially increases productivity (+10.13%) but at the expense of increased energy consumption (+15.09%). Overall, these results indicate that increasing temporal resolution in the optimization inputs shifts the optimal trade-off between productivity and energy consumption rather than delivering uniform improvements across the Pareto front. Hence, we conclude that:

$$KPI_y^*(\bar{T}_y, \overline{RH}_y, \theta_y^*) \neq \overline{\text{KPI}}_y^*(\bar{T}_{m,i}, \overline{RH}_{m,i}, \theta_{m,i}^*)$$

Table 2. Annual-mean KPI comparison for yearly-constant and monthly-constant optimization (max-Pr, min-W_{eq}). The relative KPI changes are calculated with respect to the yearly optimization strategy that produces KPI_y^* at each operating point. $\Delta\text{KPI} > 0$ signifies an increase in the measured KPI.

Operating point	Strategy	Pr	Weq	$\Delta\,\text{Pr}\,\%$	$\Delta Weq\,\%$
$Pr_{y,max}^*$	KPI_y^*	6.22	4.95	-	-
	$\overline{\text{KPI}}_y^*$	6.20	5.16	-0.37	4.35
$Weq_{y,min}^*$	KPI_y^*	3.81	2.98	-	-
	$\overline{\text{KPI}}_y^*$	4.20	3.43	10.13	15.09

Furthermore, as shown in Figure 6, by investigating the month-by-month value of re-optimization at $Pr_{y,max}^*$ we observe that monthly re-optimization yields higher productivity in most months, with $\%\Delta Pr \geq 0$ in 9 out of 12 months. The largest productivity increase occurs in January (+4.75%), while the most pronounced productivity penalty occurs in November (-6.98%), indicating that re-optimization does not consistently preserve the productivity-extreme solution across the full seasonal

envelope of monthly mean conditions. The energy response at $Pr^*_{y,max}$ is mixed and season dependent. The equivalent work decreases (i.e., $\%\Delta W_{eq} \leq 0$) in 8 out of 12 months, reaching a maximum reduction of -11.68% in April and -7.56% in May, but increases in the remaining months, with the largest penalty occurring in October (+7.79%). Consequently, monthly re-optimization at the productivity-driven operating point does not yield uniform co-improvement but instead induces month-specific trade-offs where productivity gains may be accompanied by higher energy consumption (e.g., January, October, December), and energy reductions may coincide with reduced productivity (notably November). At the minimum-energy operating point, monthly re-optimization produces a consistent productivity improvement in every month, with $\%\Delta \mathrm{Pr} > 0$ for 12 out of 12 months. The magnitude of the productivity uplift is substantial, ranging from +1.48% (March) up to +23.02% (November), demonstrating that the fixed yearly operating strategy is systematically conservative in terms of throughput when applied under month-specific ambient conditions.

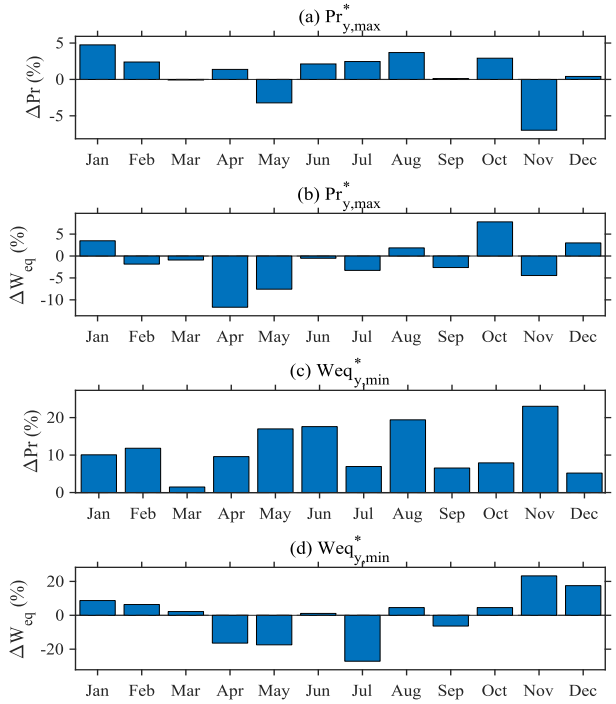


Figure 6. Monthly percentage change in productivity and equivalent work when applying monthly re-optimization relative to fixed yearly-optimized operation evaluated at $Pr^*_{y,\max}$ (a/b) and at $W^*_{\mathrm{eq},y,\min}$ (c/d).

In contrast, the energy effect remains highly seasonal. Equivalent work is reduced (i.e., $\%\Delta W_{eq} \leq 0$) in only 4 out of 12 months - specifically April (-16.42%), May (-17.44%), July (-27.12%), and September (-6.35%) - but increases in the remaining months, with pronounced penalties in November (+23.27%) and December (+17.50%). This indicates that month-specific re-optimization does not consistently minimise energy month-by-month but rather relocates the operating point along the Pareto surface in a way that frequently favours productivity increases, occasionally at the expense of higher energy demand. When averaged on an annual scale, at $Weq^*_{y,min}$, montlhy re-optimization provides a clear annual productivity increase (~11%) with a modest reduction in Weq (~2%). A similar decrease in Weq is observed at $Pr^*_{y,max}$ coupled with a marginal increase in Pr (< 1%). Hence, we conclude that:

$$KPI_{m,i}(\bar{T}_{m,i}, \overline{RH}_{m,i}, \theta^*_y) \neq KPI^*{}_{m,i}(\bar{T}_{m,i}, \overline{RH}_{m,i}, \theta^*_{m,i})$$

$$\bar{KPI}_y \neq \bar{\mathrm{KPI}}^*_y$$

The above analysis serves as a tool to depict that finer data can improve the predicted KPIs and hence show that literature-assumptions of constant weather prevents the system from reaching its maximum potential. However, these gains are achieved under the assumption of monthly fixed weather inputs. The real operational gains should be evaluated when daily weather data is propagated along with the optimal values of operating variables. Under time-resolved weather propagation, monthly scheduling provides no meaningful benefit at $Pr^*_{y,max}$, yielding negligible productivity change (+0.03%) while increasing equivalent work (+1.72%). In contrast, at $W^*_{\mathrm{eq},y,\min}$, monthly scheduling delivers a substantial productivity gain (+10.24%) but no corresponding energy reduction, with equivalent work remaining effectively unchanged (+0.18%). Overall, the 'real gains' analysis shows that improvements inferred under aggregated ambient conditions do not necessarily translate into energy savings under intra-month variability, while productivity gains persist primarily in the energy-minimization regime. Hence, we conclude that:

$$\overline{KPI}_y \neq \overline{\mathrm{KPI}}^*_y$$

CONCLUSION

To conclude, this work leverages on a previously developed high-fidelity, mechanistic, model to assess the impact of local weather variability and temporal aggregation on model predictions and real operational gains for an S-TVSA DAC unit. We show that DAC performance responds non-linearly to temperature and relative humidity. Consequently, KPIs evaluated at monthly or yearly average conditions do not reproduce true annual performance under time-resolved operation. Productivity is consistently overestimated, while electrical energy demand and equivalent work are substantially underestimated when yearly average weather inputs are used, with important implications for techno-economic

assessment, plant sizing, and system integration.

The study further shows that increasing the temporal resolution of the optimization inputs from yearly-mean to monthly-mean ambient conditions does not deliver uniform improvements in annual performance but instead repositions the optimal operating strategy along the productivity-energy trade-off surface. Month-specific optimizations can yield localized performance peaks (e.g., productivity uplift in selected months or reduced equivalent work) that can survive aggregation and deliver an improved performance on an annual scale. Importantly, operating at the energy minimization regime can offer substantial productivity gains. However, this work highlights that the value of these strategies must be assessed through dynamic evaluation: when day-to-day weather variability is propagated through the process model, the apparent benefits inferred under aggregated conditions are attenuated, and meaningful operational improvements remain confined to specific operating regimes. Collectively, these findings indicate that weather should be treated as a primary operational input for DAC design and scheduling - rather than a secondary disturbance to be averaged out if robust, region-specific deployment near industrial clusters is to be achieved. Although demonstrated here for the UK, the proposed workflow is directly transferable to other regions through substitution of site-specific meteorological datasets and deployment constraints, enabling consistent cross-regional benchmarking of DAC performance and operating strategies.

ACKNOWLEDGEMENTS

This work was funded by Graham Taylor, an alumnus of Imperial College London who left a generous gift in his will to fund research into energy policy.

AUTHOR IDENTIFIERS

Author ORCIDs:
Eleni Chalasti: 0009-0002-5835-8331
Gbemi Oluleye: 0000-0001-7753-0315
Maria M. Papathanasiou: 0000-0002-8886-0624
Ronny Pini: 0000-0002-9443-3573

REFERENCES

1. C. Science and C. Change Committee, “Assessing the Feasibility for Large-scale DACCS Deployment in the UK Climate Change Committee Assessing the Feasibility for Large-scale DACCS Deployment in the UK, ” Feb. 2025. Accessed: Oct. 02, 2025. [Online]. Available: https://www.theccc.org.uk/wp-content/uploads/2025/02/Assessing-the-Feasibility-for-Large-scale-DACCS-Deployment-in-the-UK-2.pdf
2. Ward A, Papathanasiou MM, Pini R. The impact of design and operational parameters on the optimal performance of direct air capture units using solid sorbents. Adsorption 30:1829-1848 (2024). https://doi.org/10.1007/s10450-024-00526-y
3. Cai X, Coletti MA, Sholl DS, Allen-Dumas MR. Assessing impacts of atmospheric conditions on efficiency and siting of large-scale direct air capture facilities. JACS Au 4:1883-1891 (2024). https://doi.org/10.1021/jacsau.4c00082
4. Sendi M, Bui M, Mac Dowell N, Fennell P. Geospatial analysis of regional climate impacts to accelerate cost-efficient direct air capture deployment. One Earth 5:1153-1164 (2022). https://doi.org/10.1016/j.oneear.2022.09.003
5. A. Luukkonen and J. Elfving, “Optimizing direct air capture: evaluating the impact of process parameters on productivity, energy requirement, and cost, ” 2024. [Online]. Available: https://ssrn.com/abstract=5014185
6. Jung H, Kim K, Jeong J, Jamal A, Koh DY, Lee JH. Exploring the impact of hourly variability of air condition on the efficiency of direct air capture. Chemical Engineering Journal 508:160840 (2025). https://doi.org/10.1016/j.cej.2025.160840
7. Balasubramaniam BM, Thierry PT, Lethier S, Pugnet V, Llewellyn P, Rajendran A. Process-performance of solid sorbents for direct air capture (DAC) of CO2 in optimized temperature-vacuum swing adsorption (TVSA) cycles. Chemical Engineering Journal 485:149568 (2024). https://doi.org/10.1016/j.cej.2024.149568
8. Wiegner JF, Grimm A, Weimann L, Gazzani M. Optimal design and operation of solid sorbent direct air capture processes at varying ambient conditions. Ind. Eng. Chem. Res. 61:12649-12667 (2022). https://doi.org/10.1021/acs.iecr.2c00681
9. Stampi-Bombelli V, van der Spek M, Mazzotti M. Analysis of direct capture of $${\hbox {CO}}_{2}$$ from ambient air via steam-assisted temperature–vacuum swing adsorption. Adsorption 26:1183-1197 (2020). https://doi.org/10.1007/s10450-020-00249-w
10. S. Cluster, “Ready to Deliver Industrial Decarbonisation.” [Online]. Available: www.theccc.org.uk/publication/net-zero-the-uks-contribution-to-stopping-global-warming
11. UK Met Office, “ MIDAS Open: UK daily weather observation data, v202507, ” CEDA Archive. Accessed: Jan. 08, 2026. [Online]. Available: https://data.ceda.ac.uk/badc/ukmo-midas-open/data/uk-daily-weather-obs/dataset-version-202507/

© 2026 by the authors. Licensed to PSEcommunity.org and PSE Press. This is an open access article under the creative commons CC-BY-SA licensing terms. Credit must be given to creator and adaptations must be shared under the same terms. See https://creativecommons.org/licenses/by-sa/4.0/

